

Extinction of a nonadiabatic flame propagating through spatially periodic shear flow

I. Brailovsky and G. Sivashinsky

*School of Mathematical Sciences, Sackler Faculty of Exact Sciences, Tel Aviv University, Ramat-Aviv 69978, Israel
and The Levich Institute for Physico-Chemical Hydrodynamics, The City College of New York, New York, New York 10033
(Received 22 June 1994)*

It is shown that the nonadiabatic premixed flame propagating through zero-mean, time-independent, periodic shear flow is quenched provided the flow-field intensity exceeds a certain critical level. In the nearly quenched flame at the points of its highest stretch, where the flame temperature is lowest, the stretch intensity appears to be independent of the flow scale, provided the latter is large enough. It is argued that the results obtained may be relevant to the experimentally known phenomenon of flame quenching by turbulence.

PACS number(s): 47.70.Fw, 82.40.Py

I. INTRODUCTION

An interaction between the flame and large-scale eddies of the turbulent flow field results in the extension of the flame interface and thereby in the burning rate enhancement. Yet it has long been observed that for each gaseous premixture there is a certain level of turbulence at which the speed of the premixed flame reaches its maximal value. A further increase in the flow intensity leads to a drop of the flame speed, interface fragmentation, and eventual extinction of the flame [1–12]. Figure 1 depicts the typical dependence of the flame speed on the turbulent flow intensity. It has been suggested that the phenomenon is likely to be controlled by the flame stretch [6–12]. Such an interpretation, however, needs a qualification. The stretch indeed is known to reduce the reaction rate, provided it is positive [13]. Otherwise, the

burning will be enhanced by the stretch rather than suppressed. In turbulent flow the sign of the stretch alternates along the front. Thus it is not at all clear how the inhibiting influence of the stretch occurring in some parts of the flame will dominate the other parts of the flame and result in the overall flame extinction. Moreover, there are serious indications that, while the stretch certainly plays an important role, in order to ensure the complete extinction, some level of heat losses is indispensable [14–17]. The stretch idea of flame extinction, therefore, still involves questions, the elucidation of which calls for a more fundamental approach.

The principal difficulty in modeling turbulent combustion, as in many other turbulence related problems, is the wide range of spatiotemporal scales involved. It seems intuitively plausible, however, that the multiple-scale nature of the flow field is not crucial for the physics of flame extinction which may well be described within the framework of a rather simple one-scale flame-flow interaction scheme. As has been shown in our previous studies of the problem, one may gain a good deal of apparently relevant information even when the underlying flow is chosen as time independent, space periodic, and unidirectional [17–20]. It was found that the response of the adiabatic flame speed to the gradual increase of the periodic flow intensity is rather nontrivial. For long-wavelength periodic flows there exists a certain critical amplitude above which the combustion wave undergoes a jumpwise (hysteresic) transition from a high- to a low-speed propagation mode. For gasless systems this transition may be accompanied by a partial extinction [17]. Yet complete extinction within a purely adiabatic picture does not seem feasible no matter how strong the flame distortion and stretch.

The present paper is intended as a further exploration of the issue and its extension over the case when the requirement of adiabaticity is relaxed and the pertinent model is allowed to incorporate the effects due to volumetric heat losses. It is quite understandable that strong enough heat loss may suppress any exothermic flame whether there is a background flow or not. The question is whether or not an intensive enough flow field

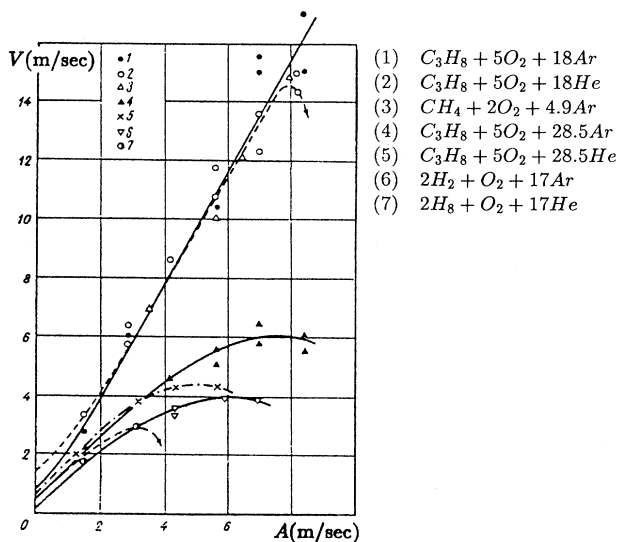


FIG. 1. Turbulent flame speed V versus turbulent flow intensity A . The level of turbulence was controlled by four high speed fans within the explosion vessel [3].

may destroy a moderately nonadiabatic flame maintainable in the quiescent premixture.

II. MATHEMATICAL MODEL

We employ the following framework for the model: a one-step irreversible reaction with Arrhenius's kinetics and large activation energy; the reactant composition is far from stoichiometric; constant density and transport properties; a time-independent, unidirectional, and periodic flow field. In the present model we also include the effect due to radiative heat loss.

With these assumptions the nondimensional set of equations for temperature and concentration in the frame of reference attached to the corrugated flame (Fig. 2) reads

$$\mathbf{v} \cdot \nabla T = \nabla^2 T + (1 - \sigma) e^{(1/2)\beta(T-1)} \delta_\varphi - h(T^4 - \sigma^4), \quad (2.1)$$

$$\mathbf{v} \cdot \nabla C = \text{Le}^{-1} \nabla^2 C - e^{(1/2)\beta(T-1)} \delta_\varphi, \quad (2.2)$$

where $\delta_\varphi = \sqrt{1 + \varphi_y^2} \delta(x - \varphi)$ is the surface δ function, $x = \varphi(y)$ is the flame interface (location of the reaction zone), and

$$\mathbf{v} = (W(ky), 0) \quad \text{with } W(ky) = V + A \cos ky. \quad (2.3)$$

Here T , β , and σ are the local, activation, and initial temperatures, respectively, in units of the adiabatic temperature of combustion products; C is the local concentration of the deficient reactant in units of its initial value in a fresh mixture; (x, y) are the spatial coordinates in units of the flame thermal width; \mathbf{v} is the flow-field velocity in units of the planar adiabatic flame speed; Le is the Lewis number. A is the prescribed amplitude (intensity) of the flow field and V is the speed of the corrugated flame, which is to be determined alongside T , C , and φ in the course of the solution of the problem. $h(T^4 - \sigma^4)$ is the term responsible for the radiative heat losses, with h being the scaled Stefan-Boltzmann constant (heat loss intensity).

In this formulation, the deficient reactant is assumed to be completely used up within the reaction zone. Hence

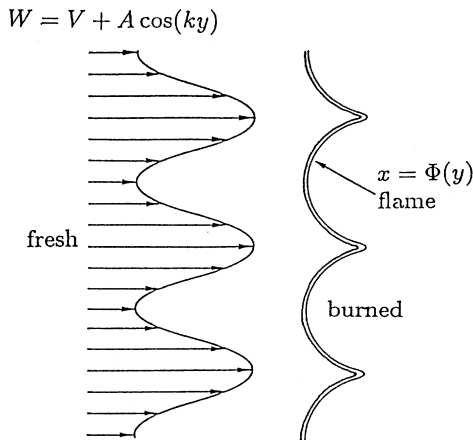


FIG. 2. Schematic view of a corrugated flame stabilized in a periodic shear flow $\mathbf{v} = (V + A \cos ky, 0)$.

$$C(x, y) = 0 \quad \text{at } x > \varphi(y). \quad (2.4)$$

Far from the reaction zone the following boundary conditions are imposed:

$$C(-\infty, y) = 1, \quad T(\pm\infty, y) = \sigma. \quad (2.5)$$

III. ASYMPTOTIC ANALYSIS

As in our previous paper [18], the problem (2.1)–(2.6) is analyzed within the framework of the so-called slowly varying flame (SVF) formulation, which, for all its inherent limitations, often proves to be the only available analytical means to tackle essentially nonlinear and multidimensional premixed flame systems.

The SVF approach is known to be most effective when the typical length scale of the flow k^{-1} is large, while the heat loss intensity h is small, and both are related to the large activation energy β as

$$k \sim h \sim \beta^{-1} \quad (\beta \gg 1). \quad (3.1)$$

It is precisely in this parameter range, as we shall see below, that the extinction of the corrugated flame occurs.

The algebra involved in SVF perturbative machinery is well known and will not be reproduced here. The interested reader may refer to some of the original papers on the subject [21–24] and the book by Buckmaster and Ludford [25]. The final asymptotic relations for the flame interface $x = \varphi(y)$ and its temperature T_F at the leading-order approximation read

$$\mu(\mathbf{v} \cdot \mathbf{n}) \frac{d}{ds} \left[\frac{\mathbf{v} \cdot \boldsymbol{\tau}}{\mathbf{v} \cdot \mathbf{n}} \right] + (\mathbf{v} \cdot \mathbf{n})^2 \ln(\mathbf{v} \cdot \mathbf{n}) + \beta h \Gamma(\sigma) = 0, \quad (3.2)$$

$$T_F = 1 + \frac{2}{\beta} \ln(\mathbf{v} \cdot \mathbf{n}). \quad (3.3)$$

Here

$$\mathbf{n} = (1, -\varphi_y) / \sqrt{1 + \varphi_y^2}, \quad \boldsymbol{\tau} = (\varphi_y, 1) / \sqrt{1 + \varphi_y^2}, \quad (3.4)$$

$$\Gamma(\sigma) = 2\sigma^3(1 - \sigma) + \frac{3}{2}\sigma^2(1 - \sigma^2) + \frac{3}{8}\sigma(1 - \sigma^3) + \frac{5}{8}(1 - \sigma^4), \quad (3.5)$$

$$\mu = \frac{1}{2}\beta(1 - \sigma)(1 - \text{Le}^{-1}) \quad (3.6)$$

is the truncated (SVF) version of the Markstein number (see, e.g., [28]).

$$K = \mu(\mathbf{v} \cdot \mathbf{n}) \frac{d}{ds} \left[\frac{\mathbf{v} \cdot \boldsymbol{\tau}}{\mathbf{v} \cdot \mathbf{n}} \right] \quad (3.7)$$

is the so-called flame stretch, characterizing the local response of the normal flame speed to the distortion of the flame structure due to its curvature and the flow-field divergence (see, e.g., [26], where one may find more general expressions pertinent to time-dependent and three-dimensional systems).

For the relations (3.2) and (3.3) to be meaningful,

$$(\mathbf{v} \cdot \mathbf{n}) = W(ky) / \sqrt{1 + \varphi_y^2} \quad (3.8)$$

should be positive. Hence

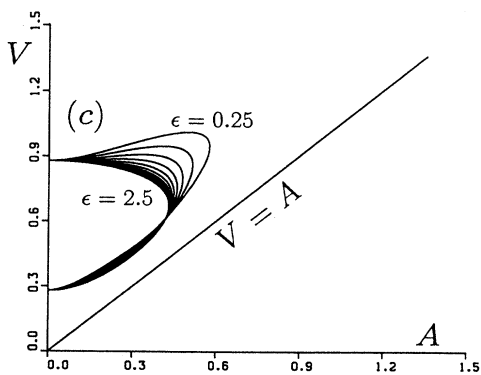
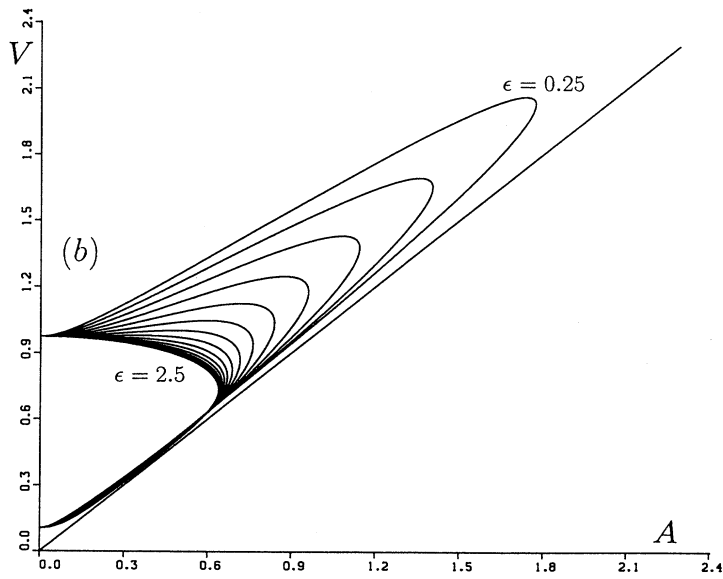
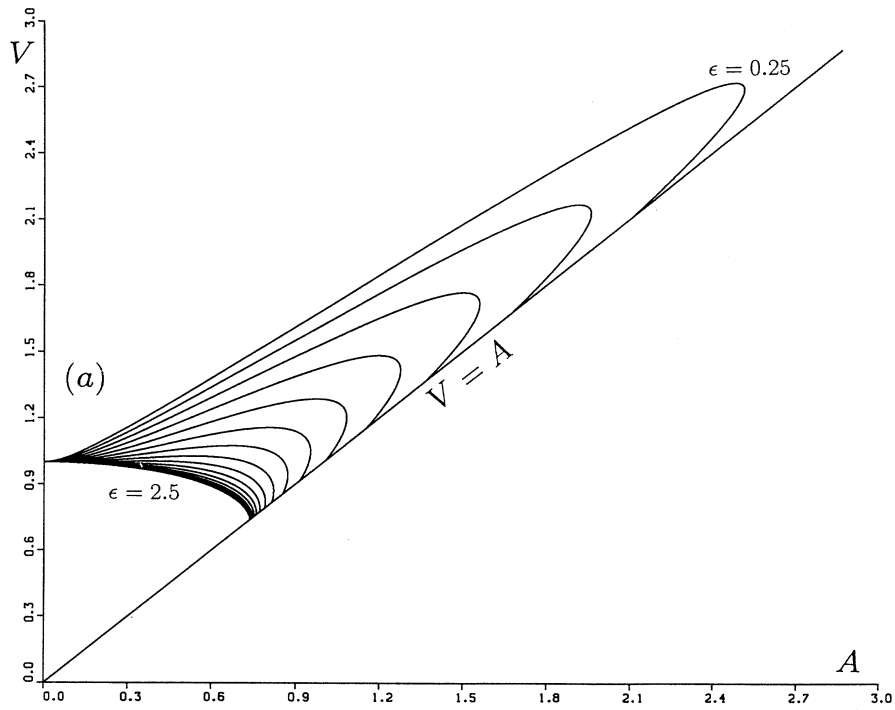


FIG. 3. Corrugated flame speed V versus periodic flow amplitude A for (a) $\alpha=0$, (b) $\alpha=0.025$, and (c) $\alpha=0.1$ at $\epsilon=\epsilon_n$ ($0 \leq n \leq N=15$), $\epsilon_0=0.25, \epsilon_N=2.5$, and $\ln \epsilon_n = (1-n/N) \ln \epsilon_0 + (n/N) \ln \epsilon_N$.

$$V > A .$$

(3.9)

profiles $\varphi(y)$ and $W(ky)$. As a result one obtains

$$\begin{aligned} \mu\varphi_{yy} &= W(ky) \ln[\sqrt{1+\varphi_y^2}/W(ky)] \\ &\quad - \beta h \Gamma[(1+\varphi_y^2)/W(ky)] , \end{aligned} \quad (3.10)$$

$$T_F = 1 - 2\beta^{-1} \ln[\sqrt{1+\varphi_y^2}/W(ky)] , \quad (3.11)$$

$$K = \mu\varphi_{yy} W(ky)/(1+\varphi_y^2) . \quad (3.12)$$

Beyond this region the equilibrium state either fails to exist or the flame interface partially moves backward towards the burned gas (negative flame speed). For the SVF formalism the latter situation is not admissible.

For further analysis it is convenient to recast (3.2), (3.3), and (3.7) in terms of the interface and velocity

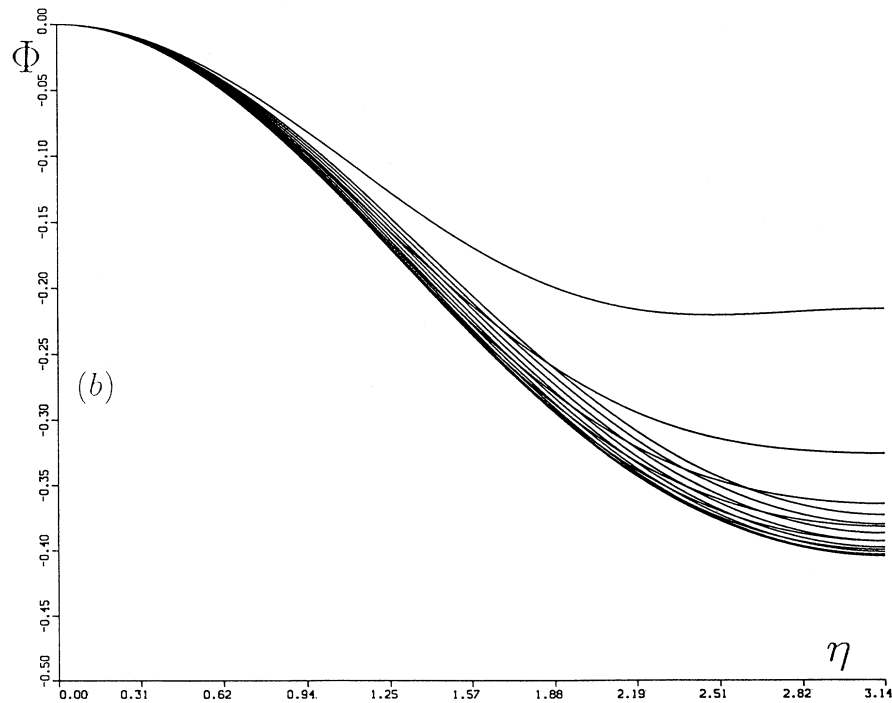
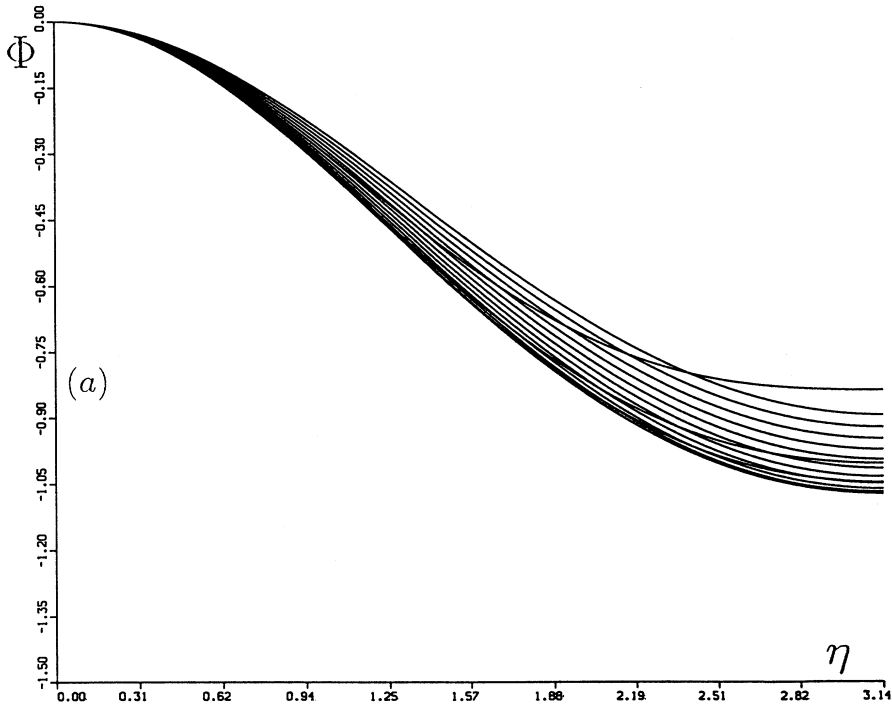


FIG. 4. Flame interface profile $\Phi(\eta)$, $0 < \eta < \pi$, for $A = A^q(1-n/50)$, $n=0,1, \dots, 15$. (a) $\alpha=0$, $\varepsilon=1$ ($A^q=0.774$, $V^q=0.789$); (b) $\alpha=0,1$, $\varepsilon=1$ ($A^q=0.433$, $V^q=0.684$). The interface is maximally extended (lower curve) at $A=0.690$, $V=0.919$ for $\alpha=0$ and at $A=0.360$, $V=0.802$ for $\alpha=0.1$.

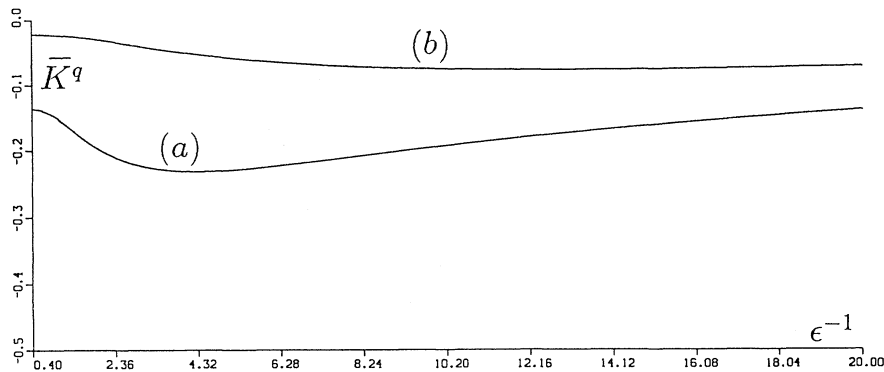


FIG. 5. Mean value of the stretch \bar{K}^q at the quenching point versus the flow length scale ϵ^{-1} for (a) $\alpha=0$ and (b) $\alpha=0.1$.

IV. EQUATION FOR THE FLAME INTERFACE AND ITS SOLUTION

Introducing the new scaled variables and parameters

$$\begin{aligned} \eta &= ky, \quad G(\eta) = \varphi_y, \\ \Theta_F &= \frac{1}{2}\beta(T_F - 1) \quad (\text{reduced flame temperature}), \\ \epsilon &= \mu k \quad (\text{scaled wave number}), \\ \alpha &= \beta h \Gamma(\sigma) \quad (\text{scaled heat loss intensity}), \end{aligned} \tag{4.1}$$

relations (3.10)–(3.12) become

$$\epsilon G_\eta = W(\eta) \ln[\sqrt{1+G^2}/W(\eta)] - \alpha(1+G^2)/W(\eta), \tag{4.2}$$

$$\Theta_F = -\ln[\sqrt{1+G^2}/W(\eta)], \tag{4.3}$$

$$K = \epsilon G_\eta W(\eta)/(1+G^2), \tag{4.4}$$

where $W(\eta) = V + A \cos \eta$. Since W_η vanishes at $\eta=0$ and π , it is natural to impose the same conditions on the flame slope $G(\eta)$ as well, i.e.,

$$G(0) = 0, \quad G(\pi) = 0. \tag{4.5}$$

The problem (4.2) and (4.5) is clearly overdetermined since here one has two boundary conditions for the first-order ordinary differential equation. Thus one ends up with a nonlinear eigenvalue problem where $V = V(A, \epsilon, \alpha)$ plays the role of the unknown parameter.

Due to its nonlinear nature, the problem (4.2) and (4.5) is not accessible to analytical treatment. Yet it may be rather efficiently solved numerically. The basic idea of the adopted computational algorithm, which is a marked improvement over the standard shooting method used in [18], is as follows.

Setting $A=0$, one integrates Eq. (4.2) subject to the initial condition $G(0)=0$ to obtain the function

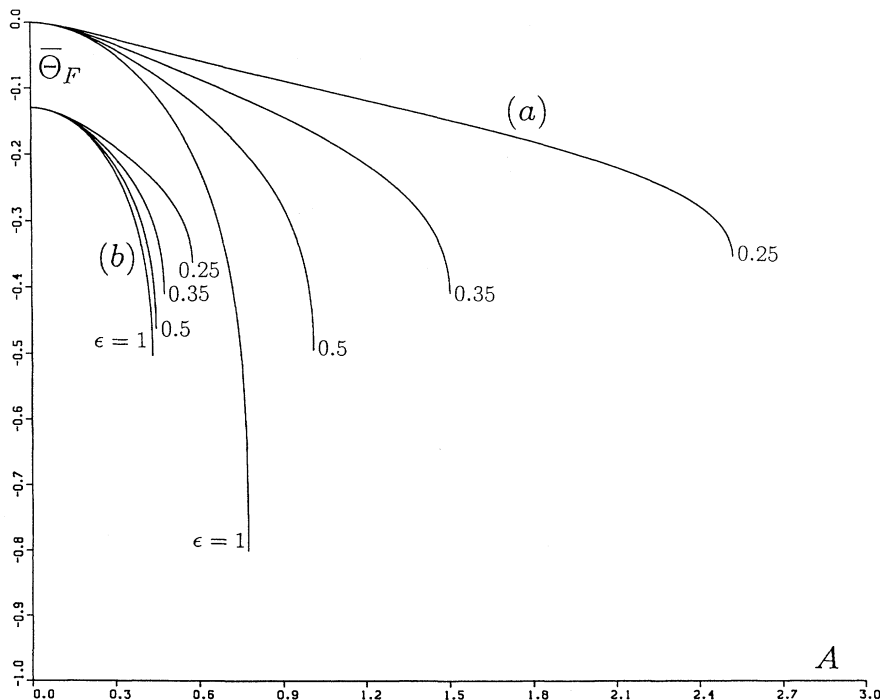


FIG. 6. Mean value of the reduced flame front temperature $\bar{\Theta}_F$ versus the periodic flow amplitude A for (a) $\alpha=0$ and (b) $\alpha=0.1$ at $\epsilon=1, 0.5, 0.35,$ and 0.25 .

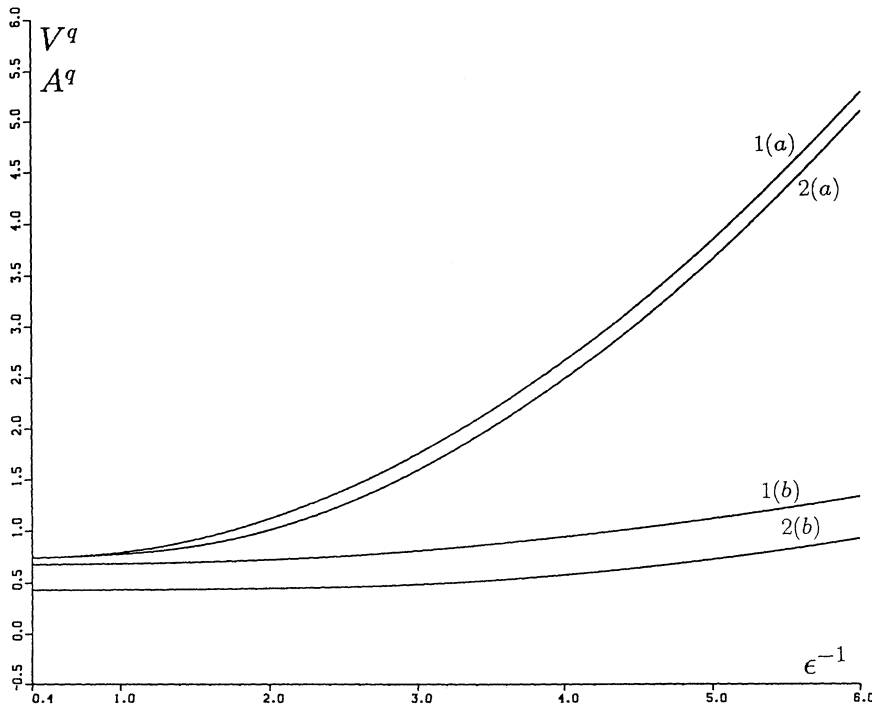


FIG. 7. Periodic flow amplitude A^q —(1) and corrugated flame speed V^q —(2) at the quenching point versus the flow length scale ϵ^{-1} for (a) $\alpha=0$ and (b) $\alpha=0.1$.

$G_v(\pi)=g(V)$. Solving the equation $g(V)=0$, one determines the intersection points between the sought for curve $R(V, A)=0$ and the axis $A=0$. These points are localized within the interval $0 < V < 1$. Thereupon, starting from the found intersections, one gradually constructs the rest of the curve $R(V, A)=0$. To ensure the desired resolution, an appropriate adaptive algorithm is employed. At small ϵ the problem (4.2) and (4.5) becomes stiff, acquiring an ϵ -wide boundary layer near $y=0$. To maintain an acceptable accuracy and without introducing too many mesh points, Eq. (4.2) was solved with a variable step.

A. The adiabatic case ($\alpha=0$)

Figure 3(a) depicts the speed V of the corrugated flame as a function of the flow intensity A for different wave numbers. For any ϵ there is a threshold (quenching point) $A^q = A^q(\epsilon)$ above which the equilibrium solution in the

region $V > A$ does not exist. Shorter-wavelength (larger- ϵ) solutions go out at lower amplitudes A than the longer-wavelength solutions. There are two solutions for each A near the quenching point. Apparently only the upper one is physically feasible (stable).

Figure 4(a) shows several flame interface configurations $\Phi(\eta) = \int_0^\eta G(\bar{\eta}) d\bar{\eta}$ for a variety of amplitudes A . Quite in keeping with the $V(A)$ dependence [Fig. 3(a)], as A increases, the flame interface initially expands and then, approaching the quenching point A^q , shrinks. At $\eta=0$, where $W = V + A$, the reduced flame temperature Θ_F (4.1) reaches its highest value (above zero), while at $\eta=\pi$, where $W = V - A$, Θ_F is lowest. For the stretch K the situation is the opposite. It is strongest at $\eta=\pi$ and weakest at $\eta=0$. For positive μ , the mean value $\bar{K}^q = \int K^q ds / \int ds$ appears to be negative and apparently gradually vanishing as $\epsilon^{-1} \rightarrow \infty$ (Fig. 5). The mean of the reduced temperature $\bar{\Theta}_F^{-1} = \int \Theta_F ds / \int ds$ is also negative

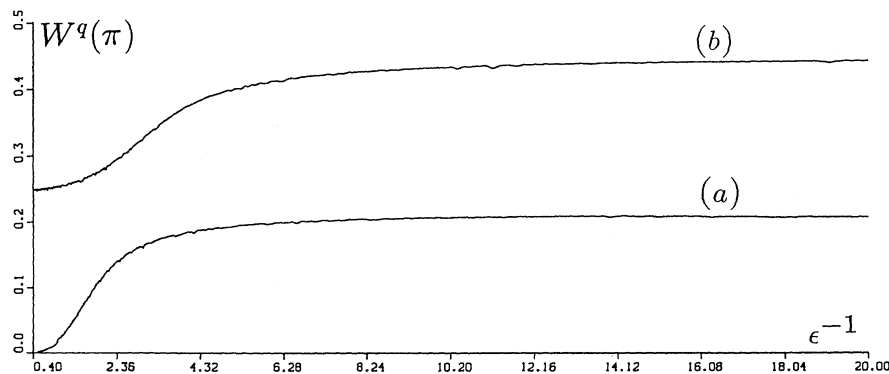


FIG. 8. Local flame speed $W^q(\pi) = V^q - A^q$ at the quenching point versus the flow length scale ϵ^{-1} for (a) $\alpha=0$ and (b) $\alpha=0.1$.

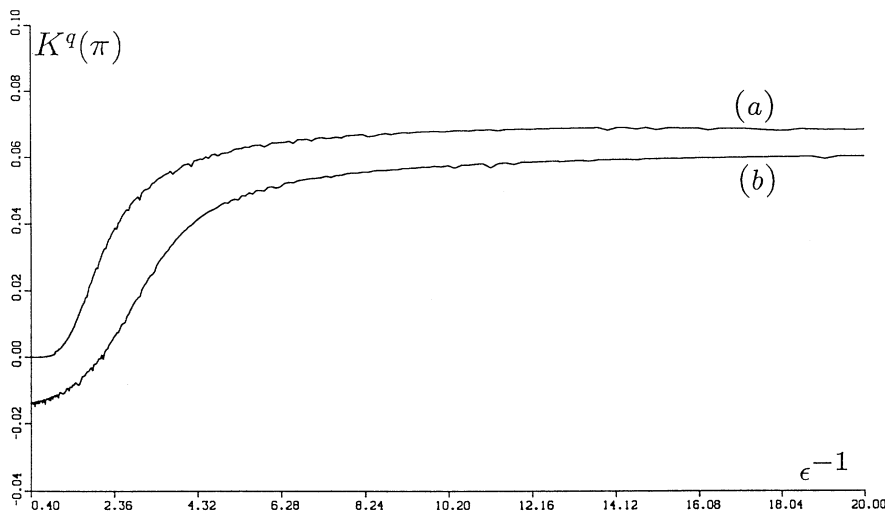


Fig. 9. Local stretch $K^q(\pi)$ at the quenching point versus the flow scale ϵ^{-1} for (a) $\alpha=0$ and (b) $\alpha=0.1$.

and rapidly drops with the increasing A (Fig. 6). Figure 7(a) yields the dependences of A and V on the flow scale ϵ^{-1} evaluated at the quenching point q . For large length scales ϵ^{-1} , at the flame's weakest point ($\eta=\pi$), the flame speed $W^q(\pi)=V^q-A^q$ and consequently the stretch $K^q(\pi)$ approach constant values, i.e., appear to be scale independent [Figs. 8(a) and 9(a)]. It is interesting that the scale independence holds not only for the quenching points A^q , but for the points of maximal stretch as well, where the stretch invariance settles even at shorter length scales [Fig. 10(a)].

B. The nonadiabatic case ($\alpha > 0$)

As one may see from Fig. 3(a), at $\alpha=0$ each of the curves $R(V, A)=0$ touches the boundary $V=A$ below which, as was mentioned earlier, the SVF formalism underlying Eq. (4.2) collapses. In fact, there is a continuous transition of each of the curves $R(V, A)=0$ into the $V < A$ region [17]. Thus, although for $A > A^q$ the SVF solution disappears from the $V > A$ region, the actual flame does not go out but merely passes to a new propa-

gation regime where at some parts of the flame its speed W relative to the underlying flow happens to be negative.

The incorporation of heat losses ($\alpha > 0$) changes the picture dramatically. Figures 11 and 3(b) show the flame speed V versus the flow intensity A for different levels of heat losses α at a fixed wave number ϵ and for different wave numbers at a fixed heat loss. Here, even for very small α the corresponding curves $R(V, A)=0$ remain entirely within the $V > A$ region. At $\alpha \rightarrow 1/2e \approx 0.18$ the curves $R(V, A)=0$ gather at the singular point $A=0$, $V=1/\sqrt{e} \approx 0.6$, which is precisely the classical flammability limit of a planar flame. In this situation reading the nonexistence as an actual extinction becomes much more credible. Additional arguments in favor of such an interpretation will be presented in the next section.

Figure 4(b) shows several interface configurations of a nonadiabatic flame. For relatively high α and ϵ at A close enough to the quenching point A^q , the flame buckles near $\eta=\pi$. While affecting the local stretch $K(\pi)$, which may change its sign, this does not cause a qualitative alternation in the temperature distribution along the

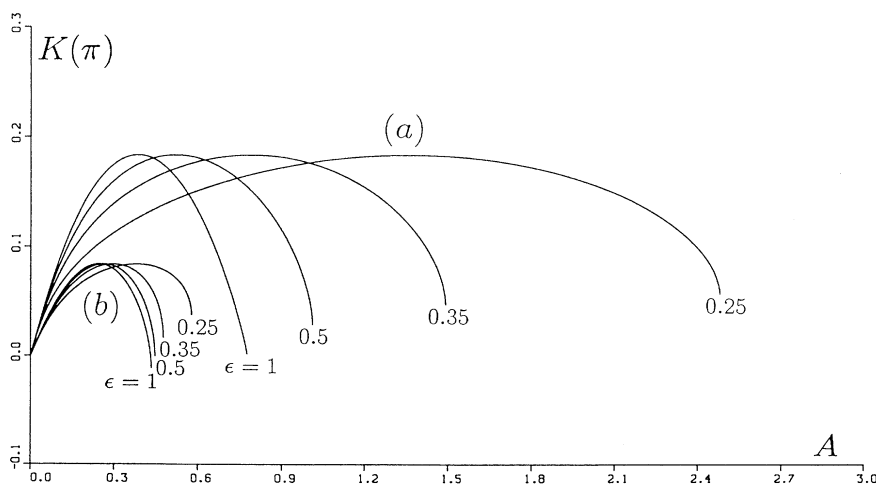


FIG. 10. Local flame stretch $K(\pi)$ versus periodic flow amplitude A for (a) $\alpha=0$ and (b) $\alpha=0.1$ at $\epsilon=1, 0.5, 0.35,$ and 0.25 .

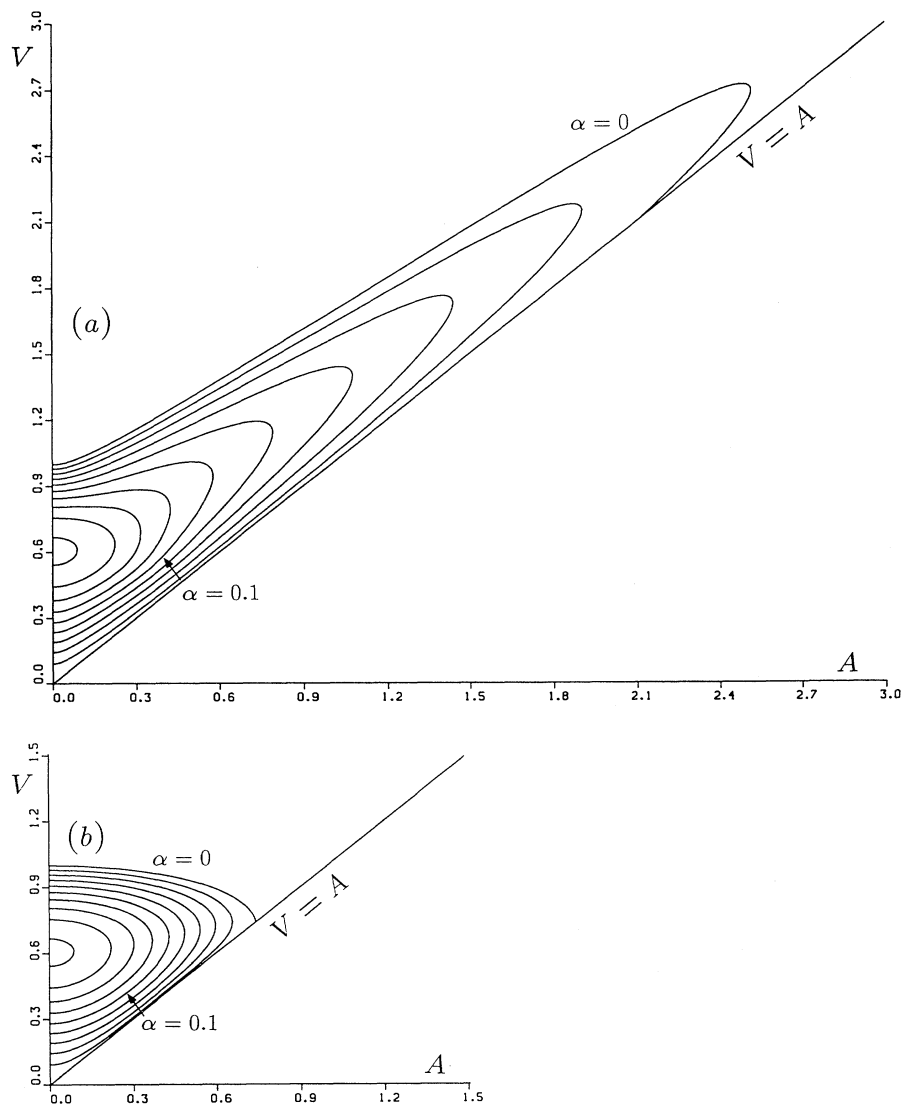


FIG. 11. Corrugated flame speed V versus periodic flow amplitude A for different levels of heat loss α at $\epsilon=0.25$ (long waves) and $\epsilon=2.5$ (short waves). $\alpha=0.02n$ ($n=0, \dots, 9$).

flame interface. Figure 6(b) shows the mean temperature drop with increasing A .

Figures 7(b), 8(b), and 9(b) present A^q , V^q , $W^q(\pi)$, and $K^q(\pi)$ versus the length scale ϵ^{-1} of $\alpha=0.1$. As in the adiabatic case, $W^q(\pi)$ and $K^q(\pi)$ become length-scale independent for larger ϵ^{-1} .

V. THE QUASI-ONE-DIMENSIONAL MODEL

Formally speaking, the found effect merely asserts the disappearance of the periodic solution of Eq. (4.2), but does not say much about what actually happens to the system beyond the existence point. Does the flame indeed go out or is the matter more involved? The most straightforward way to resolve this question is clearly through the direct numerical simulation of the pertinent reaction-diffusion system. With modern computational facilities this is quite a feasible albeit a challenging project. In this paper, however, we adopted a somewhat less rational and direct yet technically much more accessible "sandwich model" approach originally employed for the

adiabatic case [17]. In this approach, the original two-dimensional reaction-diffusion-advection system is regarded as a pile of alternately sliding reacting layers. The latter, in turn, are treated as one-dimensional systems with a volumetric mechanism of the diffusive-thermal interaction. The problem is thus reduced to a set of four spatially one-dimensional equations for T_{\pm} and C_{\pm} associated with moving layers labeled by \pm (Fig. 12).

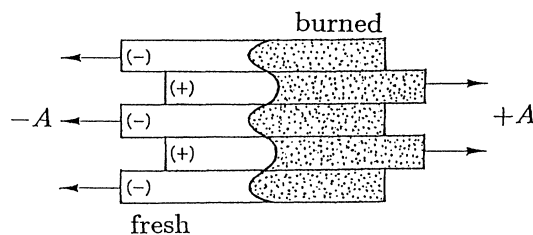


FIG. 12. Schematic view of a premixed flame moving through a pile of alternately sliding reactive layers.

To gain some idea of the possible influence of heat loss the discussion will be limited to the simplest case of "gas-less" ($Le = \infty$) combustion spreading through a pile of sliding layers of solid fuel [17]. In order not to deal with the narrow reaction zone and hopefully without much detriment to the qualitative understanding of the phenomenon, the normally exponential temperature dependence of the reaction rate is replaced by the quadratic one. Accordingly, to prevent a reaction in the cold

premixture its temperature σ is set at zero. The heat loss term is appropriately modified as well. One thus ends up with a rather compact and computationally convenient model, which at the laboratory frame of reference reads

$$\frac{\partial T_{\pm}}{\partial t} \pm A \frac{\partial T_{\pm}}{\partial x} = \frac{\partial^2 T_{\pm}}{\partial x^2} + k^2(T_{\mp} - T_{\pm}) + \Omega_{\pm} - hT_{\pm}, \quad (5.1)$$

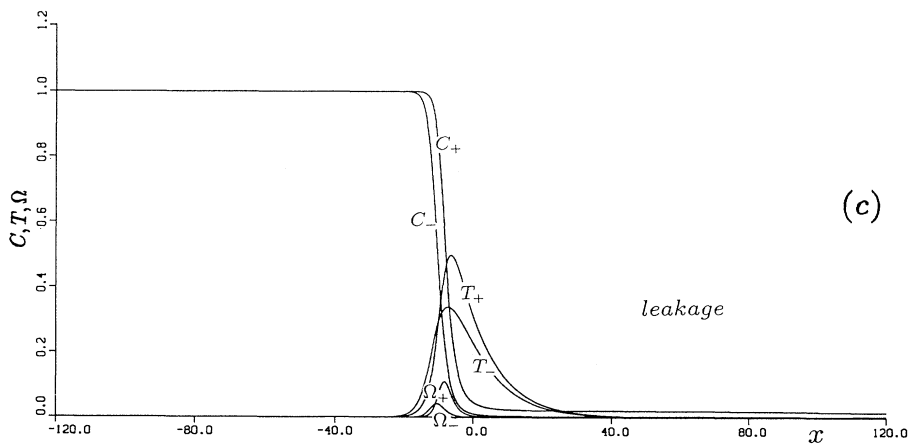
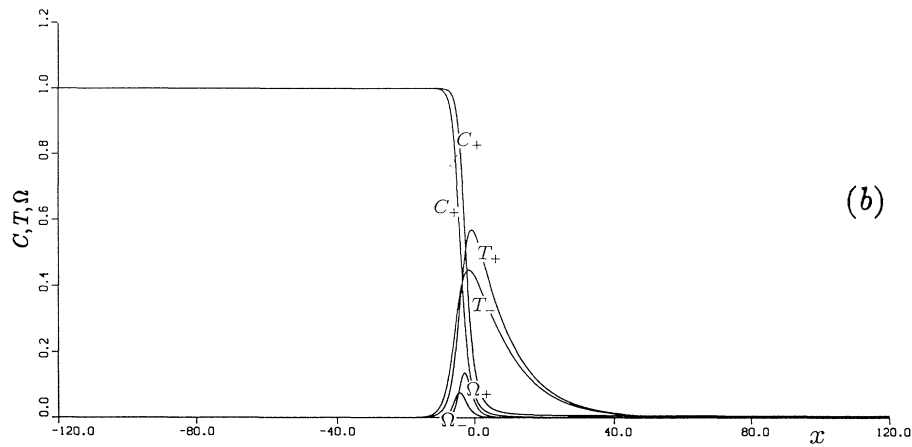
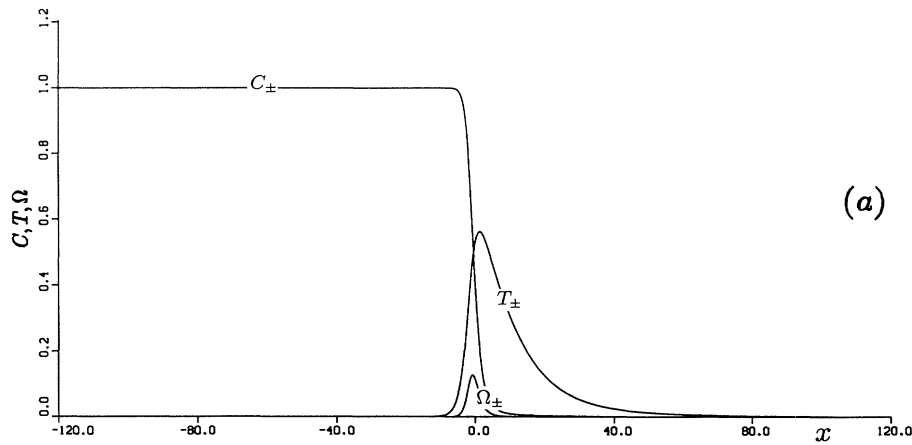


FIG. 13. Temperature T , concentration C , and reaction rate Ω profiles at $k=0.3$ and $h=0.06$ for (a) $A=0$, (b) $A=0.14$, (c) $A=0.18$, (d) $A=0.19$, and (e) $A=0.195$.

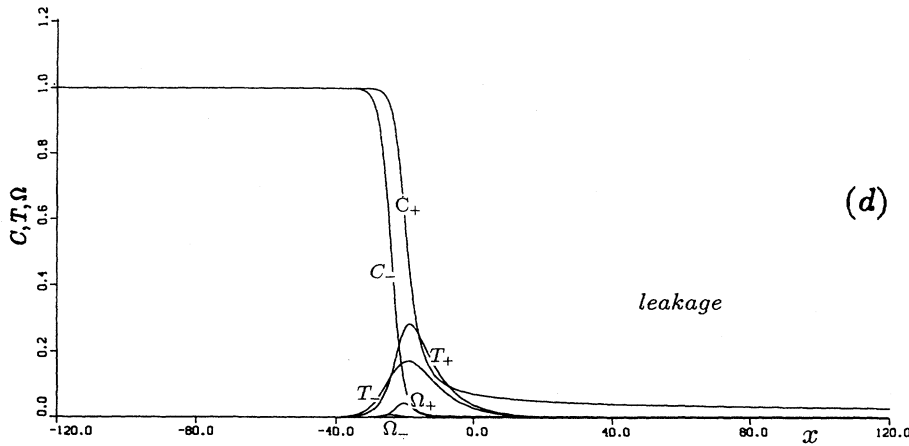
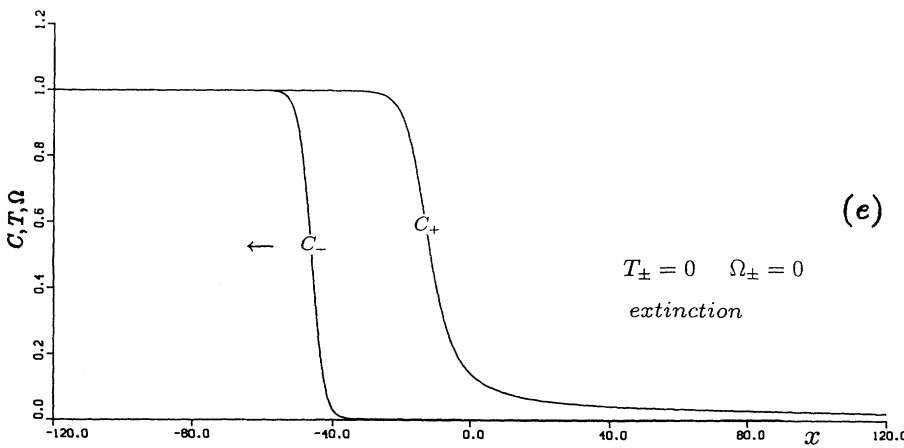


FIG. 13. (Continued).



$$\frac{\partial C_{\pm}}{\partial t} \pm A \frac{\partial C_{\pm}}{\partial x} = -\Omega_{\pm}, \quad \Omega_{\pm} = C_{\pm} T_{\pm}^2, \quad (5.2)$$

$$T_{\pm}(-\infty, t) = 0, \quad C_{\pm}(-\infty, t) = 1, \quad (5.3)$$

$$\frac{\partial T_{\pm}}{\partial x} (+\infty, t) = 0, \quad \frac{\partial C_{\pm}}{\partial x} (+\infty, t) = 0. \quad (5.4)$$

At $A = 0$ the reaction waves in both layers (\pm) are clearly identical. The corresponding profiles of temperature T_{\pm} , concentration C_{\pm} , and reaction rate Ω_{\pm} are shown in Fig. 13(a). Under the mild shear A the profiles split [Fig. 13(b)] and the overall flame appears to be concave relative to the fresh mixture in the $+$ layers, where the flame moves against the stream ($+A$), and convex in the $-$ layers, where the flame moves down the stream ($-A$). The reaction rate is enhanced at the concave ($+$) and depleted at the convex ($-$) parts of the front.

At moderately strong shear one can clearly identify the reactant C_{+} leakage through the front [Fig. 13(c)]. As A increases, the leakage becomes stronger [Fig. 13(d)], while the reaction rates Ω_{\pm} noticeably weaken, and above a certain threshold A^q the reaction in both layers goes out completely [Fig. 13(e)]. Thus, at least in the chosen parameter range the nonadiabatic flame may indeed be suppressed by the background shear flow, provided its intensity is high enough. Since up to the quenching point

C_{-} does not leak, the speed V of a well settled flame may be determined from the relation [17]

$$V = A + \int_{-\infty}^{+\infty} \Omega_{-} dx. \quad (5.5)$$

In accordance with the analytical results (Fig. 11), depending on the wave number k and the level of heat losses h , the flame speed at the quenching point may be lower or higher than that of a planar flame (Fig. 14). At $h = 0.06$ for a planar flame [$A = 0$, Fig. 13(a)] $V = 0.57$. The planar flame goes out at $h^q = 0.08$, $V^q = 0.43$. For $h = 0.06$, $k = 0.3$ the flame goes out at $A^q = 0.194$, $V^q = 0.42$. For $h = 0.05$, $k = 0.1$ the flame goes out at $A^q = 0.297$, $V^q = 0.84$. For $k = 0.3$ and sufficiently weak heat losses (e.g., $h = 0.02$) the behavior of the system is qualitatively similar to that of the adiabatic flame [17]: above a certain critical shear $A^q = 0.5$, the flame undergoes partial extinction, yet does not go out completely.

VI. DISCUSSION AND CONCLUDING REMARKS

The one-scale flame-flow interaction scheme discussed in this paper appears to be quite adequate to capture the basic aspects of flow-induced quenching. It seems plausible to suggest that the local scale independence of the Lagrangian stretch (3.7) at the quenching point found for periodic shear flows has the same nature as the scale in-

dependence of the mean Eulerian stretch ($\lambda^{-1}U_{\text{rms}}^q$) occurring in turbulent systems [7–12]. Here U_{rms}^q is the turbulent flow quenching intensity and λ is its Taylor length scale. Yet the nearly quadratic dependence between the shear flow intensity A^q and the “Taylor length scale” $\lambda = U_{\text{rms}}/(U_y)_{\text{rms}} = k^{-1}$ (Fig. 7) is markedly different from what is actually observed in turbulent flames where the measurements are shown to correlate with the estimate $U_{\text{rms}} \sim \lambda$ [7–12]. The concrete realization of the quenching, therefore, seems to be rather sensitive to whether the flow field is isotopic and multiple scale or not. To clarify the point the SVF formulation still may be an appropriate framework. The issue will be addressed in a future study.

The disappearance of the continuous SVF solutions at $A = A^q$ generally does not imply that the actual flame will be quenched simultaneously along the whole interface. What is found here is perhaps the incipient stage preceding the extinction. For instance, the employed model rules out the possibility of leakage, which seems to be a rather characteristic feature of the near-limit combustion. The observed nonexistence, therefore, may well

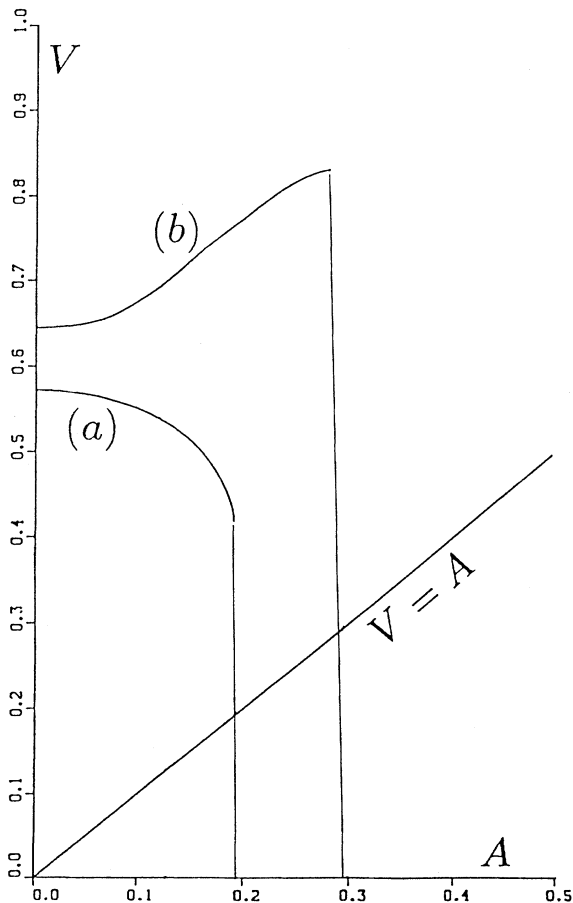


FIG. 14. Flame speed V versus shear intensity A at (a) $k = 0.3$, $h = 0.06$ and (b) $k = 0.1$, $h = 0.05$.

be merely a signal sent by the model that the nonleakage condition becomes too restrictive and should be relaxed. To clarify this point it would be instructive to carry out a straightforward numerical simulation of the original model similar to those recently undertaken for the related reaction-diffusion systems (e.g., [14,16,27]).

The observed sensitivity of the model (4.2) and (4.3) to the presence of even a minute heat loss is clearly nothing but a by-product of the SVF formalism based on the large β (activation energy) limit. In more realistic models employing large but finite β , the phenomenology of adiabatic and nearly adiabatic flames will hardly be distinguishable. Note that even in the framework of the SVF asymptotics, the flammability limit $A^q(\epsilon, \alpha)$ of a nearly adiabatic system ($\alpha \ll 1$) practically coincides with the turning point of the adiabatic system $A^q(\epsilon, \alpha = 0)$. The latter therefore may well provide relevant information on the actual flammability limit, which in principle is unfeasible without heat losses.

The parameter $\epsilon = \frac{1}{2}\beta k(1 - \sigma)(1 - \text{Le}^{-1})$ appearing in Eq. (4.2) may be positive as well as negative. The corresponding solutions $G(\eta)$ will differ only by their signs. On physical grounds, however, the case of positive ϵ , i.e., $\text{Le} > 1$, is in a sense safer. The point is that at negative ϵ ($\text{Le} < 1$) the system (2.1)–(2.5) is susceptible to the so-called diffusive-thermal (cellular) instability (see, e.g., [28]), not covered by the SVF formalism. The actual phenomenology of the flame-flow interaction may thus prove to be more complicated here than is allowed by the present theory. Indeed, it was observed that rich hydrocarbon mixtures ($\text{Le} < 1$) are more difficult to quench than lean ones ($\text{Le} > 1$), with an opposite effect for H_2 mixtures [5,8]. Yet, for relatively narrow domains where the flame is intrinsically stable there seems to be quite a good correlation between Eq. (4.2) and the system (2.1)–(2.5), irrespective of the sign of ϵ [29].

The SVF formulation is relevant only if the Lewis number (Le) is not too close to unity. The similarity case $\text{Le} = 1$ requires an independent investigation. For the adiabatic system it has been shown that there is always a solution for any amplitude A , however large [30,31]. This outcome is quite understandable physically. At $\text{Le} = 1$, in the absence of heat losses, distortion of the flame front does not affect its temperature and therefore may not lead to the flame extinction. It was also found in the above studies that $W(ky)$, being positive on average, may well change sign along the front, thereby exhibiting the negative-flame-speed effect. The latter seems to be rather characteristic for the system irrespective of its Lewis number.

The range of validity of the sandwich model employed in Sec. V, formally speaking, is limited to large k , permitting replacement of the derivative T_{yy} by the appropriate finite difference. Yet it appears that the obtained quasi-one-dimensional model yields a qualitatively reasonable phenomenology not only for large, but for moderately small k as well [17]. It is not, however, the case for very small k , where the interaction between the sliding nonadiabatic layers weakens and they may become too independent to move in tandem. This is exactly what happens if one takes, for example, $k = 0.05$, $h = 0.06$.

ACKNOWLEDGMENTS

This research was supported in part by the U.S. Department of Energy under Grant No. DE-FG02-

88ER1382, by the National Science Foundation under Grant No. CTS-9213414, and by the U.S.–Israel Binational Science Foundation under Grant No. 93-00030.

-
- [1] N. F. Coward and G. W. Jones, U.S. Bur. Mines **503**, 1 (1952).
- [2] V. P. Karpov and A. S. Sokolik, Dokl. Akad. Nauk. SSSR **141**, 866 (1961) [Sov. Phys. Dokl. **141**, 393 (1961)].
- [3] A. S. Sokolik, V. P. Karpov, and E. S. Semenov, Combust. Explos. Shock Waves (USSR) **3**, 36 (1967).
- [4] R. G. Abdel-Gayed, D. Bradley, and M. McMahon, in *Seventeenth Symposium (International) on Combustion* (The Combustion Institute, Pittsburgh, 1979), pp. 245–254.
- [5] V. P. Karpov and E. S. Severin, Combust. Explos. Shock Waves **16**, 41 (1980).
- [6] J. Chomiak and J. Jarosinsky, Combust. Flame **48**, 241 (1982).
- [7] R. G. Abdel-Gayed, K. J. Al-Khishali, and D. Bradley, Proc. R. Soc. London Ser. A **391**, 393 (1984).
- [8] R. G. Abdel-Gayed, D. Bradley, M. N. Hamid, and M. Lawes, in *Twentieth Symposium (International) on Combustion* (The Combustion Institute, Pittsburgh, 1984), pp. 505–512.
- [9] R. G. Abdel-Gayed and D. Bradley, Combust. Flame **62**, 61 (1985).
- [10] R. G. Abdel-Gayed, D. Bradley, and M. Lawes, Proc. R. Soc. London Ser. A **414**, 389 (1987).
- [11] R. G. Abdel-Gayed, D. Bradley, and A. K. C. Lau, in *Twenty-Second Symposium (International) on Combustion* (The Combustion Institute, Pittsburgh, 1988), pp. 731–738.
- [12] R. G. Abdel-Gayed and D. Bradley, Combust. Flame **76**, 213 (1989).
- [13] F. A. Williams, *Combustion Theory*, 2nd. ed. (Benjamin/Cummings, Menlo Park, CA, 1985).
- [14] T. Poinso, D. Veynante, and S. Candel, J. Fluid Mech. **228**, 561 (1991).
- [15] B. D. Haslam and P. D. Ronney, in *Fall Technical Meeting, Western States Section* (The Combustion Institute, Berkeley, 1992).
- [16] G. Kozlovsky and G. I. Sivashinsky, Theor. Comput. Fluid Mech. **6**, 181 (1994).
- [17] I. Brailovsky and G. I. Sivashinsky, Combust. Sci. Technol. **95**, 51 (1994).
- [18] H. Berestycki and G. I. Sivashinsky, SIAM J. Appl. Math. **51**, 344 (1991).
- [19] R. C. Aldredge, Combust. Flame **90**, 121 (1992).
- [20] K. M. Yu, C. K. Law, and C. J. Sung, Combust. Flame (to be published).
- [21] G. I. Sivashinsky, J. Chem. Phys. **62**, 638 (1975).
- [22] G. I. Sivashinsky, Acta Astron. **3**, 889 (1976).
- [23] J. D. Buckmaster, Combust. Flame **28**, 225 (1977).
- [24] P. Ronney and G. I. Sivashinsky, SIAM J. Appl. Math. **49**, 1029 (1989).
- [25] J. D. Buckmaster and G. S. S. Ludford, *Theory of Laminar Flames* (Cambridge University Press, Cambridge, 1982).
- [26] M. Matalon, Combust. Sci. Technol. **31**, 169 (1983).
- [27] F. Benkhaldoun, B. Denet, and B. Larrouturou, Combust. Sci. Technol. **69**, 187 (1984).
- [28] G. I. Sivashinsky, Philos. Trans. R. Soc. London Sect. A **332**, 135 (1990).
- [29] G. Kozlovsky and G. I. Sivashinsky (unpublished).
- [30] H. Berestycki and B. Larrouturou, Z. Rein. Angew. Math. **396**, 14 (1989).
- [31] H. Berestycki, B. Larrouturou, and P. L. Lions, Arch. Rat. Mech. Anal. **111**, 33 (1990).